ELSEVIER

European Journal of Pharmacology 447 (2002) 279–284

www.elsevier.com/locate/ejphar

L-type Ca^{2+} channels of the embryonic mouse heart

Norbert Klugbauer *, Andrea Welling, Verena Specht, Claudia Seisenberger, Franz Hofmann

Institut für Pharmakologie und Toxikologie der Technischen Universität München, Biedersteiner Str. 29, 80802 Munich, Germany

Accepted 15 April 2002

Abstract

In the heart, where Ca^{2+} influx across the sarcolemma is essential for contraction, L-type Ca^{2+} channels represent the major entry pathway of Ca^{2+}. Mice with a homozygous deletion of the L-type $Ca_v1.2$ Ca^{2+} channel gene die before day 14.5 p.c. Electrophysiological and pharmacological investigations on $Ca_v1.2-/-$ cardiomyocytes demonstrated that contractions depended on the influx of Ca^{2+} through an L-type-like Ca^{2+} channel. We analyzed now the expression pattern of various L-type Ca^{2+} channels. Amplification of the alternative exons 1a and 1b revealed that embryonic cardiac cells express both $Ca_v1.2a$ and $Ca_v1.2b$ subunits. Reverse transcriptase-polymerase chain reaction (RT-PCR) amplifications indicated the expression of $Ca_v1.1$ and $Ca_v1.3$ in about a 1:10 ratio in $Ca_v1.2-/-$ embryos. Two different amino termini of the $Ca_v1.3$ cDNA were found in the embryonic heart, which both gave rise to functional channels. $Ca_v1.3(1a)$ and $Ca_v1.3(1b)$ channels have similar current kinetics and voltage-dependencies as described for $Ca_v1.3_{8A}$ channels [J. Biol. Chem. 276 (2001) 22100], but the properties of $Ca_v1.3(1a)$ or $Ca_v1.3(1b)$ channels are different from that of the L-type-like current in $Ca_v1.2-/-$ cardiomyocytes. The I_{Ba} of $Ca_v1.3(1a)$ was blocked by the dihydropyridine nisoldipine with an IC_{50} value of 0.13 μM at a holding potential of −80 mV. In embryonic $Ca_v1.2+/+$ cardiomyocytes, I_{Ba} was blocked by nisoldipine with an IC_{50} value of 0.1 μM. Although the expressed $Ca_v1.3$ channel has a similar affinity for nisoldipine as $Ca_v1.2+/+$ cardiomyocytes, the L-type-like Ca^{2+} channel found in $Ca_v1.2+/+$ and $-/-$ cardiomyocytes is not identical with the new $Ca_v1.3$ splice variants.

Keywords: Ca^{2+} channel, voltage-gated; $Ca_v1.3$; L-type Ca^{2+} channel; Embryo, mouse; Heart; Dihydropyridine

1. Introduction

Ca^{2+} ions play a crucial role in the excitation and contraction of the heart. Ca^{2+} is a ubiquitous second messenger that is essential in cardiac electrical activity and is the direct activator of the myofilaments, which finally cause contraction. During the cardiac action potential, Ca^{2+} influx in ventricular myocytes occurs through voltage-activated Ca^{2+} channels thereby contributing to its plateau phase. Myocytes exhibit two families of voltage-activated Ca^{2+} channels: L-type and T-type. Ca^{2+} influx through T-type channels is negligible in most ventricular myocytes, but is important in the sinoatrial node region where $Ca_v3.1$, a T-type Ca^{2+} channel, is expressed at high density (Bohn et al., 2000). L-type channels are generally considered to be important for Ca^{2+} influx in the working myocard. These channels are located primarily at the sarcolemmal-sarcoplasmic reticulum junctions, where the ryanodine receptors exist. The L-type Ca^{2+} channels comprise a family of four members, namely $Ca_v1.1$ to $Ca_v1.4$ (reviewed in Hofmann et al., 1999). $Ca_v1.1$ has been cloned so far only from skeletal muscle, but two reports described the detection of skeletal muscle Ca^{2+} channel subunits in cultured neonatal cardiac myocytes (Haase et al., 1994; Mejia-Alvarez et al., 1994). $Ca_v1.2$ is expressed in heart, smooth muscle, pancreas, adrenal gland and brain. This channel has been considered to be the major L-type channel in the heart. $Ca_v1.3$ is mainly found in brain, but also in pancreas, kidney, ovary and cochlea. $Ca_v1.3$ transcripts have also been detected in cardiac tissues (Yaney et al., 1992; Takimoto et al., 1997; Wyatt et al., 1997). $Ca_v1.4$ has been identified only in the retina (Bech-Hansen et al., 1998).

Mouse knockout models are a valuable tool to unravel the different physiological functions of L-type Ca^{2+} channels in the heart (Seisenberger et al., 2000; Platzer et al., 2000). Homozygous $Ca_v1.2-/-$ mice die before day 14.5 p.c. probably due to the lack of functional $Ca_v1.2$ in the heart. This assumption is further confirmed by a mutation in the $Ca_v1.2$ gene in zebra fish (Rottbauer et al., 2001). Again, deletion of this channel is lethal and leads to a selective

* Corresponding author. Tel.: +49-89-4140-3256; fax: +49-89-4140-3261.

E-mail address: klugbauer@ipt.med.tu-muenchen.de (N. Klugbauer).

0014-2999/02/$ - see front matter © 2002 Elsevier Science B.V. All rights reserved.
PII: S0014-2999(02)01850-2

perturbation of cardiac morphogenesis and function in early embryonic development. Deletion of $Ca_v1.3$ led to sinoatrial node bradycardia and arrythmia, indicating a functional role of the $Ca_v1.3$ channel in cardiac rhythmogenesis (Platzer et al., 2000).

The aim of this study was to analyze the expression of various L-type Ca^{2+} channels and some of their splice variants in embryonic hearts.

2. Expression of $Ca_v1.2$ splice variants in the embryonic heart

Tissue specific expression of several splice variants of the $Ca_v1.2$ gene has been described (Welling et al., 1997). The $Ca_v1.2a$ splice variant is expressed in the heart, $Ca_v1.2b$ in smooth muscle and $Ca_v1.2c$ predominantly in brain (Hofmann et al., 1999). These splice variants differ only at four sites, namely the amino terminus, the transmembrane segments IS6 and IVS6 and an insert in the cytoplasmic loop connecting repeat I and II, which is only present in the $Ca_v1.2b$ subunit. Transient expression of the different amino terminal splice variants revealed that constructs with the $Ca_v1.2a$ amino terminus had low I_{Ba} densities, whereas constructs with the $Ca_v1.2b$ amino terminus had intermediate or high current densities (Welling et al., 1997). Furthermore, the $Ca_v1.2b$ channel has a higher affinity for dihydropyridines than the $Ca_v1.2a$ channel. In order to identify which of the splice variants of $Ca_v1.2$ is expressed in day 12.5 p.c. wild type mouse embryos, primers specific for either exon1a or exon1b were used. The amplification with these exon-specific primers revealed that embryonic heart expresses both exons (Fig. 1). In brain and in the remaining part of the embryo, only the $Ca_v1.2b$ amino terminus was found. Transcripts of these exons were not identified in the hearts of $Ca_v1.2-/-$ embryos since the neomycin cassette was inserted in exon 3 (Seisenberger et al., 2000). These results suggest that embryonic cardiac cells may express the "cardiac-" and the "smooth muscle-" specific $Ca_v1.2$ channel at embryonic day 12.5. However,

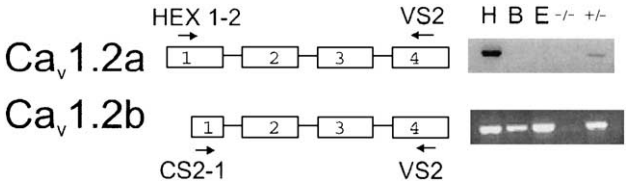

Fig. 1. Reverse transcriptase-polymerase chain reaction (RT-PCR) amplification of mRNA from murine embryonic tissue preparations at day 12.5 p.c. Left part: scheme of exons 1–4 of $Ca_v1.2a$ and $Ca_v1.2b$ mRNA. HEX1-2 is a primer specific for the amino terminus of $Ca_v1.2a$ and CS2-1 specific for the amino terminus of $Ca_v1.2b$. Right part: RT-PCR amplification of mRNA from wild type (H, B and E) heterozygous (+/−) and homozygous (−/−) $Ca_v1.2$ embryos. mRNA was isolated from heart (H), brain (B), remaining part of the embryo (E) and total embryos (+/−; −/−).

the $Ca_v1.2$ channel cannot be of functional importance since the deletion of the gene encoding $Ca_v1.2$ indicated that (1) mouse embryos develop apparently normal up to day 12.5 p.c. in the absence of the intact $Ca_v1.2$ gene. (2) Hearts are able to contract in the absence of $Ca_v1.2$ at day 12.5 p.c. (3) Cardiac contraction requires influx of Ca^{2+} through an L-type-like Ca^{2+} channel. (4) In $Ca_v1.2-/-$ cardiomyocytes, an I_{Ba} with L-type-like kinetics and pharmacology was identified. (5) The molecular identity of this L-type-like channel is unknown (Seisenberger et al., 2000).

3. Identification of L-type Ca^{2+} channels in the embryonic heart by reverse transcriptase-polymerase chain reaction (RT-PCR) amplification

In order to identify the molecular structure of this apparent L-type Ca^{2+} current, degenerate primers were designed that were specific for all known L-type Ca^{2+} channel sequences. These primers were used for RT-PCR amplification of cardiac RNA from day 12.5 p.c. −/− embryos. To avoid the amplification of $Ca_v1.2$ sequences, mouse strain B was used in which exons 14 and 15 were deleted (Seisenberger et al., 2000). In each amplification reaction, one primer was located in the region of deletion. DNA fragments obtained by this protocol were separated on an agarose gel, cut out and cloned. The clones were characterized by sequencing and by restriction analysis. $Ca_v1.1$ and $Ca_v1.3$ DNA fragments were found in a 1:10 ratio. No other Ca^{2+} channel gene was identified. It was very unlikely that the L-type-like Ba^{2+} current of the $Ca_v1.2-/-$ hearts was caused by the $Ca_v1.1$ skeletal muscle channel because the kinetics of the murine $Ca_v1.1$ channel and the cardiac L-type-like Ba^{2+} current differed significantly (Strube et al., 2000).

Although unlikely, it was possible that the cardiac L-type-like Ba^{2+} current was caused by a splice variant of the $Ca_v1.3$ gene. As a first step, the $Ca_v1.3$ channel was cloned from heart of day 12.5 p.c. $Ca_v1.2-/-$ mouse embryos by RT-PCR using the proofreading high fidelity polymerase (Fig. 2). Two alternative amino termini were identified that were termed $Ca_v1.3(1a)$ and $Ca_v1.3(1b)$. $Ca_v1.3(1a)$ corresponds to exon 1a, described previously by several authors (Williams et al., 1992; Hui et al., 1991; Seino et al., 1992), whereas $Ca_v1.3(1b)$ is transcribed from a novel exon 1b (Fig. 2A). Exon 1a encodes 22 amino acid residues, whereas exon 1b encodes for 44 amino acid residues but does not contain the characteristic seven methionines of exon 1a. The start ATG in exon 1b has a Kozak sequence with a G at pos. −3 and an A at pos. +4, which are both in accordance with high expression levels in eucaryotic cells. A database search using exon 1b showed the existence of several expressed sequence tags (ESTs) that were identical with exon 1b in the overlapping regions. These additional clones also confirmed that the putative start ATG is the first ATG downstream of an in-frame stop codon.

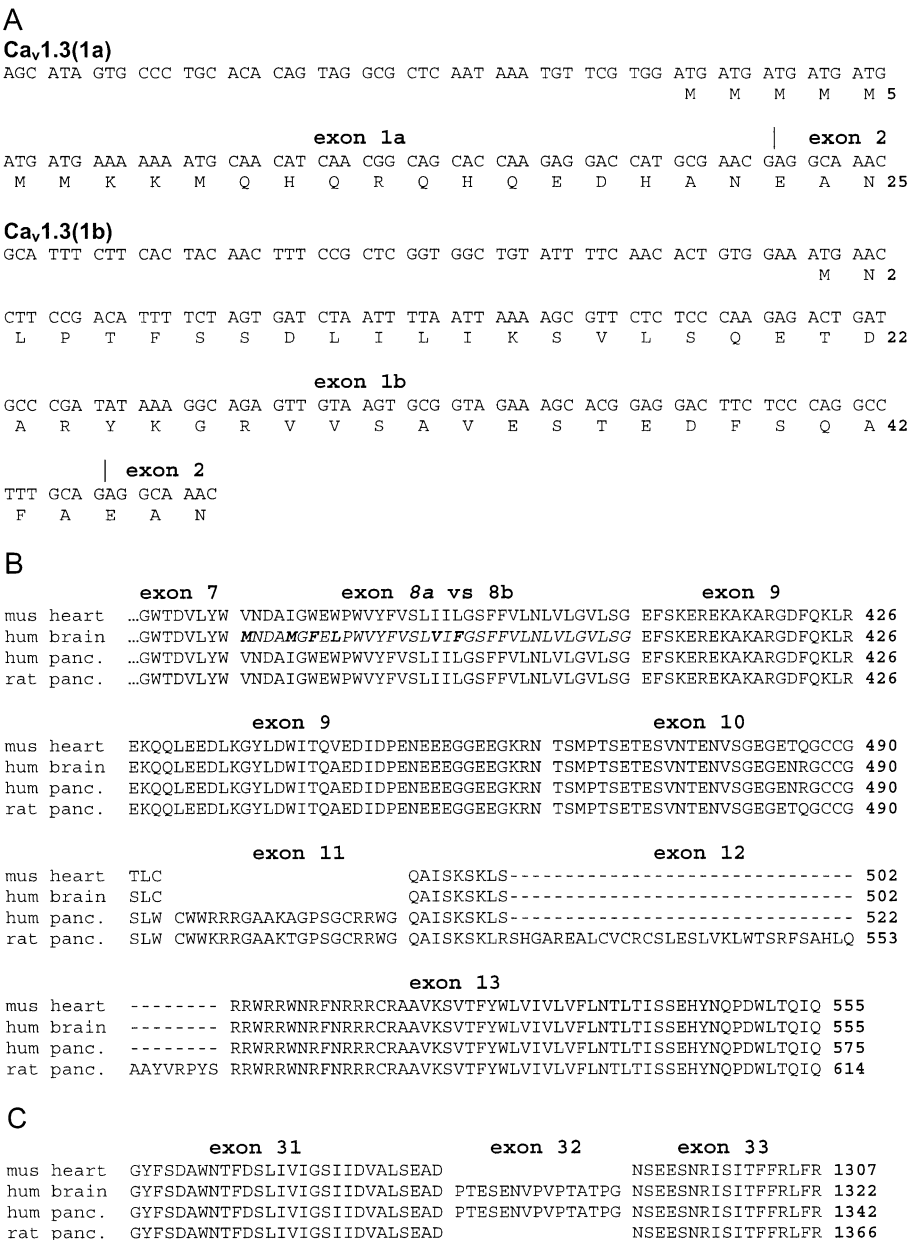

Fig. 2. Comparison of murine, human and rat $Ca_v1.3$ sequences. (A) Alternative exons 1a and 1b of the $Ca_v1.3$ mRNA. Top—nucleotide and amino acid sequence of the $Ca_v1.3(1a)$ splice variant. Bottom—nucleotide and amino acid sequence of the novel $Ca_v1.3(1b)$ splice variant. | indicates the conjunction between exons 1 and 2. (B–C) Comparison of alternative splicing in the $Ca_v1.3$ mRNA from different tissues and species: mus heart—murine embryonic heart $Ca_v1.3(1a)$; hum brain—human brain $Ca_v1.3$ cDNA cloned by Williams et al. (1992); hum panc—human pancreas $Ca_v1.3$ cDNA described by Seino et al. (1992) (please note that the cDNA from human pancreas cloned by Koschak et al. (2001) lacks exon 32); rat panc—rat pancreas $Ca_v1.3$ cDNA described by Ihara et al. (1995) (please note that RT-PCR amplifications indicated that cDNAs including exon 32 can also be detected in rat pancreas). The alternative exon 8a is printed in italics and the differences between exons 8a and 8b are indicated in bold. The full-length murine cardiac cDNA of $Ca_v1.3$ was cloned by PCR using the proofreading polymerase High Fidelity PCR enzyme (Roche). The amino terminal fragment was obtained by rapid amplification of cDNA ends (RACE).

The $Ca_v1.3$ sequence was further confirmed by additional RT-PCR reactions on channel regions between exons 7 and 13 and exons 31 and 33 that are known to be spliced differently in various tissues (Safa et al., 2001). With the exception of the two different amino termini, no additional splice variants were identified in embryonic hearts (Fig. 2B and C).

4. Electrophysiological properties of the two $Ca_v1.3$ splice variants

The two alternative splice variants were used to construct full-length $Ca_v1.3(1a)$ and $Ca_v1.3(1b)$ expression vectors. We examined the functional properties of $Ca_v1.3(1a)$ and $Ca_v1.3(1b)$ subunits by introducing their cDNAs with

accompanying β_3 and $\alpha_2\delta$-1 expression vectors in human embryonic kidney (HEK) 293 cells. Currents were recorded using the whole-cell patch-clamp technique with Ba^{2+} as the charge carrier. Heterologous expression of both cDNA plasmids in HEK293 cells yielded L-type Ba^{2+} currents. The expression efficiency of $Ca_v1.3(1b)$ was weaker compared with $Ca_v1.3(1a)$. Expression of $Ca_v1.3(1a)$ yielded a high current density in the presence of 5 mM Ba^{2+} as charge carrier (Fig. 3A and B; Table 1). The activation kinetics were fast for both splice variants. The inactivation for $Ca_v1.3(1a)$ was slow. Inactivation was even slower for $Ca_v1.3(1b)$ (Fig. 3A). The Ba^{2+} inward currents (I_{Ba}) were activated at about -40 mV and reached their maximum at potentials between -10 and 0 mV (Fig. 3B). The activation at relatively hyperpolarized membrane potentials and the slow inactivation kinetics were comparable to native and expressed $Ca_v1.3$ channels (Platzer et al., 2000; Koschak et al., 2001; Scholze et al., 2001; Xu and Lipscombe, 2001).

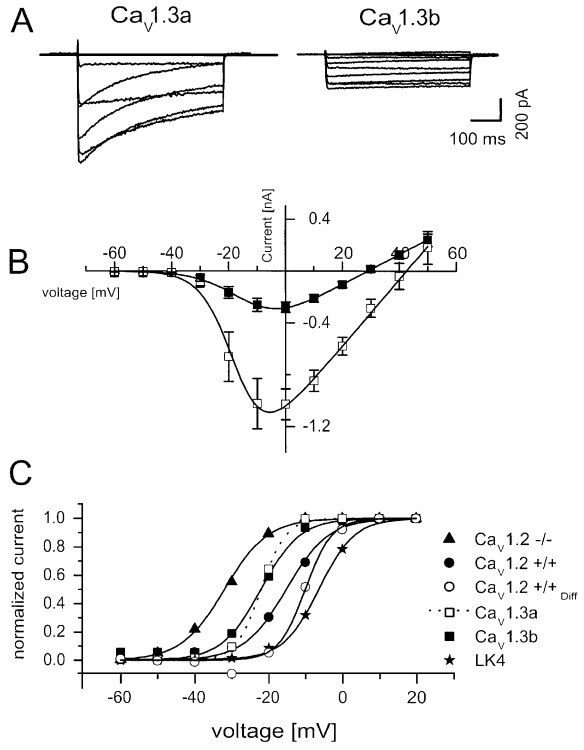

Fig. 3. Kinetics of native and expressed L-type I_{Ba}. A and B show results obtained with $Ca_v1.3(1a)$ and $Ca_v1.3(1b)$ channels transiently expressed in HEK293 cells. (A) Representative current traces to potentials from -30 to $+20$ mV ($Ca_v1.3(1a)$; 10-mV increments) or from -40 to $+40$ mV ($Ca_v1.3(1b)$; 10-mV increments) from an HP of -80 mV. (B) Averaged current voltage (I–V) relations ($Ca_v1.3(1a)$, $n=4$; $Ca_v1.3(1b)$, $n=6$). The HP was -80 mV. (C) Activation curves for expressed $Ca_v1.3(1a)$, $Ca_v1.3(1b)$ and LK4 channels and native $Ca_v1.2+/+$ and $Ca_v1.2-/-$ channels. Channels were transiently expressed in HEK293 cells together with β_3 and $\alpha_2\delta$-1 subunits. Native channels were measured in primary embryonic cardiomyocytes cultured at day 12.5 p.c. The activation curves were calculated from the averaged (I–V) relations and fitted with a Boltzmann equation. The values for $Ca_v1.2+/+_{diff}$ were determined after subtraction of the average current–voltage relationship for $Ca_v1.2-/-$ from that of $Ca_v1.2+/+$. For values, see Table 1 and for experimental details, see Seisenberger et al. (2000).

Table 1
Biophysical properties of native and expressed L-type Ca^{2+} channels

	Current density (pA/pF)	$V_{0.5,act}$ (mV)	k_{act}	V_{max} (mV)	Activation threshold
$Ca_V1.2+/+$	32 ± 2.2 (65)	−15	−5.8	+4	−32
$Ca_V1.2-/-$	13 ± 1.9 (57)	−32	−6.0	−10	−48
$Ca_V1.2+/+_{diff}$	n.d.	−10	−3.6	+6	−21
LK4	15 ± 7.1 (7)	−6	−6.0	+12	−21
$Ca_V1.3(1a)$	10 ± 1.9 (15)	−22	−3.4	−4	−37
$Ca_V1.3(1b)$	3 ± 0.7 (7)	−22	−5.3	−3	−32

The half-maximal voltage for activation ($V_{0.5,act}$), the slope for activation (k_{act}), the maximum of the current–voltage relationship (V_{max}), the activation threshold and the current densities were taken from averaged activation curves or current–voltage relations (unless stated otherwise, n = 4–6). The activation threshold was determined as the test potential at which 5% of maximal I_{Ba} was activated. The values for $Ca_V1.2+/+_{diff}$ were determined after subtraction of the average current–voltage relationship for $Ca_V1.2-/-$ from that of $Ca_V1.2+/+$.

The properties of the expressed channels were compared with recombinant channels formed by the expression of cDNAs encoding the chimeric LK4 subunit together with β_3 and $\alpha_2\delta$-1 subunits in HEK 293 cells. Chimera LK4 contains the amino terminus of the "smooth muscle"-type $Ca_v1.2b$ channel. The remaining sequence is that of the "cardiac"-type $Ca_v1.2a$ channel (Welling et al., 1997). This chimera combines a high expression efficiency with the characteristics of a cardiac $Ca_v1.2a$ channel (Welling et al., 1997). Fig. 3C compares the voltage-dependence of activation for the various channels. $Ca_v1.3(1a)$ and $Ca_v1.3(1b)$ channels had identical $V_{0.5,act}$ values of -22 mV. The most depolarized activation curve was measured for expressed $Ca_v1.2$ channel chimera LK4 with a $V_{0.5,act}$ value of -6 mV. The $V_{0.5,act}$ value (-15 mV) of the native embryonic $Ca_v1.2+/+$ current was intermediate between LK4 and $Ca_v1.3$, whereas the $V_{0.5,act}$ was -32 mV for the $Ca_v1.2-/-$ current. The slope of activation was similar for $Ca_v1.2+/+$, LK4, $Ca_v1.3(1b)$ and $Ca_v1.2-/-$ with $k=-6$. The only exception was $Ca_v1.3(1a)$ with a slope of $k=-3.4$ (Table 1). The I_{Ba} measured in $Ca_v1.2+/+$ cells is composed of several currents since after deletion of the $Ca_v1.2$ gene, an L-type-like Ca^{2+} current remained detectably in $Ca_v1.2-/-$ cardiomyocytes. Therefore, the averaged current–voltage relation from $Ca_v1.2-/-$ cells was subtracted from that of $Ca_v1.2+/+$ cells and the difference activation curve was calculated ($Ca_v1.2+/+_{diff}$). The activation curve of $Ca_v1.2+/+_{diff}$ resembles that of LK4 with $V_{0.5,act}$ of -10 versus -6 mV (Fig. 3C). The voltage-dependence of activation for I_{Ba} of $Ca_v1.3(1a)$ and $Ca_v1.3(1b)$ was shifted by -12 to -16 mV to more hyperpolarized potentials than that measured in native and expressed $Ca_v1.2$ channels. This is in good agreement with Koschak et al. (2001) who described a shift of about 14 mV. A similar shift was found for the activation threshold and the maximum of the current–voltage relationship (V_{max}). These results are summarized in Table 1 and indicate that

the currents resulting from expression of either $Ca_v1.3(1a)$ or $Ca_v1.3(1b)$ are not identical with the current measured in $Ca_v1.2-/-$ cardiomyocytes.

5. Pharmacological characterization of the L-type Ca^{2+} channels by the dihydropyridine nisoldipine

Another characteristic of the I_{Ba} of $Ca_v1.2-/-$ cardiomyocytes is its inhibition by the dihydropyridine nisoldipine at micromolar concentrations. A low dihydropyridine affinity was reported for the $Ca_v1.3$ channels (Koschak et al., 2001; Xu and Lipscombe, 2001). Therefore, we measured the nisoldipine sensitivity for the native I_{Ba} and the expressed $Ca_v1.3(1a)$ and LK4 channels (Fig. 4). These experiments were done at a negative holding potential of −80 mV to prevent voltage-dependent inhibition. The curves were fitted to the Hill equation. The dose–inhibition curve measured for expressed $Ca_v1.3(1a)$ channels corresponds well to that of native embryonic $Ca_v1.2+/+$ channels with IC_{50} values of 0.13 versus 0.1 μM. The only difference was that the curve for the inhibition of the $Ca_v1.3(1a)$ channel could be fitted by a single Hill function. The $Ca_v1.2+/+$ curve is obviously an ensemble of different currents and needed a two-component Hill function. In contrast, LK4 Ca^{2+} channels were blocked with an IC_{50} value of 0.024 μM. This value is in accordance with an IC_{50} value of 0.01 μM determined previously for $Ca_v1.2+/+$ channels expressed in murine cardiomyocytes in the late embryonic state after day 14 p.c. (Seisenberger et al., 2000). These values suggest that the $Ca_v1.2$ channel is expressed and functional in early embryonic murine cardiomyocytes

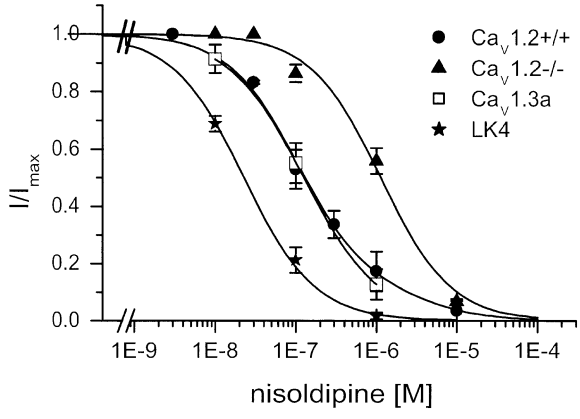

Fig. 4. Nisoldipine block of I_{Ba} from native and expressed L-type Ca^{2+} channels. L-type Ca^{2+} channels were expressed and measured as given in Fig. 3. Trains of test pulses were from −80 mV to the maximum current at 0.1 or 0.2 Hz. Data points are the mean ± S.E.M. ($n = 5–8$ cells per point). The data for $Ca_v1.2+/+$ cardiomyocytes were fitted with a two-component Hill equation, whereas data for $Ca_v1.2-/-$ cardiomyocytes, $Ca_v1.3(1a)$ and LK4 were fitted with a one-component Hill equation. The Hill coefficients are 1. The lines are the fits obtained by the Hill equation with IC_{50} values of 0.1 and 3.9 μM for $Ca_v1.2+/+$ cells (●); 1.1 μM for $Ca_v1.2-/-$ cells (▲); 0.13 μM for $Ca_v1.3(1a)$ cells (□); 0.024 μM for LK4 cells (★).

and that the L-type-like current of $Ca_v1.2-/-$ cardiomyocytes is not caused by the identified $Ca_v1.3$ channels.

6. Functional implications of the $Ca_v1.3$ splice variants

$Ca_v1.3$ transcripts were found in $Ca_v1.2-/-$ hearts by RT-PCR amplification. We cloned the full-length $Ca_v1.3$ cDNA from $Ca_v1.2-/-$ embryonic hearts. The rapid amplification of cDNA ends (RACE) cloning strategy revealed two alternative amino termini of the $Ca_v1.3$ subunit. Alternative splicing of $Ca_v1.3$ has been described so far in hair cells of the chicken's cochlea (Kollmar et al., 1997). The $Ca_v1.3$ mRNA in hair cells contains three uncommon exons. The first is a 26 amino acid insert in the cytoplasmic loop between repeats I and II, the second is an alternative exon for the transmembrane segment IIIS2 and the third is a 10 amino acid insert in the cytoplasmic loop between segments IVS2 and IVS3. It has been postulated that the alternative splicing of $Ca_v1.3$ contributes to the unusual behaviour of the Ca^{2+} channels found in the hair cell (Kollmar et al., 1997). Further splice variants were described in human and rat pancreas and some other tissues (Seino et al., 1992; Ihara et al., 1995; Koschak et al., 2001; Safa et al., 2001). The cDNA clone from human pancreas described by Koschak et al. lacks exons 32 and 44 but have alternative sequences for exon 8, which encodes the IS6 transmembrane segment. These authors could not observe any current or detect intact $Ca_v1.3$ protein in tsA-201 cells when full-length cDNA was used that included exon 8B. The cDNA from mouse embryonic heart also lacks exon 32, but contains only exon 8B. However, in contrast to the cDNA from human pancreas, the $Ca_v1.3(1a)$ and $Ca_v1.3(1b)$ cDNA induced I_{Ba} in HEK293 cells. Therefore, we conclude that the presence of exon 8B is not the only molecular switch that modulates $Ca_v1.3$ expression. Presumably, variations in other regions, like the amino terminus or the loop between repeats I and II (exons 9–12) (Williams et al., 1992; Hui et al., 1991; Seino et al., 1992; Kollmar et al., 1997), contribute to the expression of the $Ca_v1.3$ transcripts. The mouse embryonic heart $Ca_v1.3$ channel lacks exon 11, which is absent also in the human and rat brain channel (Hui et al., 1991; Williams et al., 1992).

7. Conclusions

The aim of this study was to analyze the L-type Ca^{2+} channels expressed in the early embryonic heart and to characterize these channels by heterologous expression. We took advantage of the $Ca_v1.2-/-$ embryos which do not express a functional $Ca_v1.2$ channel. In these mice, $Ca_v1.3$ was found to be the predominant L-type Ca^{2+} channel by RT-PCR analysis. RT-PCR amplification yielded also $Ca_v1.1$ transcripts at a low level. The latter observation is consistent with results obtained from cultured neonatal

cardiac myocytes (Haase et al., 1994; Mejia-Alvarez et al., 1994). The significance of the $Ca_v1.1$ transcripts is unclear because the electrophysiological characteristics of $Ca_v1.1$ such as the slow activation kinetics and the activation at positive membrane potentials were not observed in the embryonic cardiomyocytes (Seisenberger et al., 2000).

The biophysical properties of expressed $Ca_v1.3$ channels were compared with that of the native channels in embryonic cardiac myocytes. These results show that (1) the current kinetics, voltage-dependencies and dihydropyridine sensitivity of the expressed $Ca_v1.2$ and native wild type L-type channel are similar or identical; (2) $Ca_v1.3$(1a) and $Ca_v1.3$(1b) channels have similar current kinetics and voltage-dependencies as described for $Ca_v1.3_{8A}$ channels (Koschak et al., 2001); and (3) the properties of $Ca_v1.3$(1a) or $Ca_v1.3$(1b) channels are different from that of the L-type-like current in $Ca_v1.2-/-$ cardiomyocytes. In agreement with previous results (Seisenberger et al., 2000; Platzer et al., 2000), the new findings do not support an involvement of $Ca_v1.3$ in the generation of cardiac rhythm in the developing heart. The channel responsible for the inward Ba^{2+} current in murine embryonic $Ca_v1.2-/-$ cardiomyocytes remains to be identified.

Acknowledgements

We are grateful to Mrs. S. Kampf and Mrs. H.S. Lefrank for excellent technical assistance. The experimental work was supported by the Deutsche Forschungsgemeinschaft (SFB 391) and Fond der Chemischen Industrie.

References

Bech-Hansen, N.T., Naylor, M.J., Maybaum, T.A., Pearce, W.G., Koop, B., Fishman, G.A., Mets, M., Musarella, M.A., Boycott, K.M., 1998. Loss-of-function mutations in a calcium-channel alpha1 subunit gene in Xp11.23 cause incomplete X-linked congenital stationary night blindness. Nat. Genet. 19, 264–267.

Bohn, G., Moosmang, S., Conrad, H., Ludwig, A., Hofmann, F., Klugbauer, N., 2000. Expression of T- and L-type calcium channel mRNA in murine sinoatrial node. FEBS Lett. 481, 73–76.

Haase, H., Wallukat, G., Flockerzi, V., Nastaincyk, W., Hofmann, F., 1994. Detection of skeletal muscle calcium channel subunits in cultured neonatal rat cardiac myocytes. Recept. Channels 2, 41–52.

Hofmann, F., Lacinova, L., Klugbauer, N., 1999. Voltage-dependent calcium channels: from structure to function. Rev. Physiol., Biochem. Pharmacol. 139, 33–86.

Hui, A., Ellinor, P.T., Krizanova, O., Wang, J.J., Diebold, R., Schwartz, A., 1991. Molecular cloning of multiple subtypes of a novel rat brain isoform of the α_1 subunit of the voltage-dependent calcium channel. Neuron 7, 35–44.

Ihara, Y., Yamada, Y., Fujii, Y., Gonoi, T., Yano, H., Yasuda, K., Inagaki, N., Seino, Y., Seino, S., 1995. Molecular diversity and functional characterization of voltage-dependent calcium channels (CACN4) expressed in pancreatic β-cells. Mol. Endocrinol. 9, 121–130.

Kollmar, R., Fak, J., Montgomery, L.G., Hudspeth, A.J., 1997. Hair cell specific splicing of mRNA for the α_{1D} subunit of voltage-gated Ca^{2+} channels in the chicken's cochlea. Proc. Natl. Acad. Sci. U. S. A. 94, 14889–14893.

Koschak, A., Reimer, D., Huber, I., Grabner, M., Glossmann, H., Engel, J., Striessnig, J., 2001. α_{1D} ($Ca_v1.3$) subunits can form L-type Ca^{2+} channels activating at negative voltages. J. Biol. Chem. 276, 22100–22106.

Mejia-Alvarez, R., Tomaselli, G.F., Marban, E., 1994. Simultaneous expression of cardiac and skeletal muscle isoforms of the L-type Ca^{2+} channel in a rat heart muscle cell line. J. Physiol. (Lond.) 478, 315–329.

Platzer, J., Engel, J., Schrott-Fischer, A., Stephan, K., Bova, S., Chen, H., Zheng, H., Striessnig, J., 2000. Congenital deafness and sinoatrial node dysfunction in mice lacking class D L-type Ca^{2+} channels. Cell 102, 89–97.

Rottbauer, W., Baker, K., Galen Wo, Z., Mohideen, M.-A.P.K., Cantiello, H.F., Fishman, M.C., 2001. Growth and function of the embryonic heart depend upon the cardiac-specific L-type calcium channel a1 subunit. Dev. Cell 1, 265–275.

Safa, P., Boulter, J., Hales, T.G., 2001. Functional properties of $Ca_v1.3$ (alpha1D) L-type Ca^{2+} channel splice variants expressed by rat brain and neuroendocrine GH3 cells. J. Biol. Chem. 276, 38727–38737.

Scholze, A., Plant, T.D., Dolphin, A.C., Nürnberg, B., 2001. Functional expression and characterization of a voltage-gated $Ca_V1.3$ (α_{1D})calcium channel subunit from an insulin-secreting cell line. Mol. Endocrinol. 15, 1211–1221.

Seino, S., Chen, L., Seino, M., Blondel, O., Takeda, J., Johnson, J.H., Bell, G.I., 1992. Cloning of the α1 subunit of a voltage-dependent calcium channel expressed in pancreatic β cells. Proc. Natl. Acad. Sci. U. S. A. 89, 584–588.

Seisenberger, C., Specht, V., Welling, A., Platzer, J., Pfeifer, A., Kühbandner, S., Striessnig, J., Klugbauer, N., Feil, R., Hofmann, F., 2000. Functional embryonic cardiomyocytes after disruption of the L-type α_{1C} ($Ca_v1.2$) calcium channel gene in the mouse. J. Biol. Chem. 275, 39193–39199.

Strube, C., Tourneur, Y., Ojeda, C., 2000. Functional expression of the L-type calcium channel in mice skeletal muscle during prenatal myogenesis. Biophys. J. 78, 1282–1292.

Takimoto, K., Li, D., Nerbonne, J.M., Levitan, E.S., 1997. Distribution, splicing and glucocorticoid-induced expression of cardiac alpha 1C and alpha 1D voltage-gated Ca^{2+} channel mRNAsMol. Cell. Cardiol. 29, 3035–3042.

Welling, A., Ludwig, A., Zimmer, S., Klugbauer, N., Flockerzi, V., Hofmann, F., 1997. Alternatively spliced IS6 segments of the α_{1C} gene determine the tissue-specific dihydropyridine sensitivity of cardiac and vascular smooth muscle L-type Ca^{2+} channels. Circ. Res. 81, 526–532.

Williams, M.E., Feldman, D.H., McCue, A.F., Brenner, R., Velicelebi, G., Ellis, S.B., Harpold, M.M., 1992. Structure and functional expression of α_1, α_2, and β subunits of a novel human neuronal calcium channel subtype. Neuron 8, 71–84.

Wyatt, C.N., Campbell, V., Brodbeck, J., Brice, N.L., Page, K.M., Berrow, N.S., Brickley, K., Terracciano, C.M., Naqvi, R.U., MacLeod, K.T., Dolphin, A.C., 1997. Voltage-dependent binding and calcium channel current inhibition by an anti-alpha 1D subunit antibody in rat dorsal root ganglion neurones and guinea-pig myocytes [published erratum appears in J. Physiol. (Lond.) 1997 Sep 15; 503 (Pt 3) :699]. J. Physiol. (Lond.) 502, 307–319.

Xu, W., Lipscombe, D., 2001. Neuronal $Ca_v1.3$ L-type channels activate at relatively hyperpolarized membrane potentials and are incompletely inhibited by dihydropyridines. J. Neurosci. 21, 5944–5951.

Yaney, G.C., Wheeler, M.B., Wie, X., Perez-Reyes, E., Birnbaumer, L., Boyd, A.E., Moss, L.G., 1992. Cloning of a novel alpha 1-subunit of the voltage-dependent calcium channel from the beta-cell. Mol. Endocrinol. 6, 2143–2145.